Fluctuations in out of equilibrium systems: from theory to experiment

Sergio Ciliberto, Sylvain Joubaud, Artem Petrosyan

▶ **To cite this version:**

Sergio Ciliberto, Sylvain Joubaud, Artem Petrosyan. Fluctuations in out of equilibrium systems: from theory to experiment. JSTAT, 2011, P12003, pp.10. ensl-00518064v2

HAL Id: ensl-00518064

https://ens-lyon.hal.science/ensl-00518064v2

Submitted on 27 Oct 2010

HAL is a multi-disciplinary open access archive for the deposit and dissemination of scientific research documents, whether they are published or not. The documents may come from teaching and research institutions in France or abroad, or from public or private research centers.

L'archive ouverte pluridisciplinaire **HAL**, est destinée au dépôt et à la diffusion de documents scientifiques de niveau recherche, publiés ou non, émanant des établissements d'enseignement et de recherche français ou étrangers, des laboratoires publics ou privés.

Fluctuations in out of equilibrium systems: from theory to experiment

S. Ciliberto, S. Joubaud, A. Petrosyan
Université de Lyon
Ecole Normale Supérieure de Lyon, Laboratoire de Physique ,
C.N.R.S. UMR5672,
46, Allée d'Italie, 69364 Lyon Cedex 07, France

October 27, 2010

Abstract

We introduce from an experimental point of view the main concepts of fluctuation theorems for work, heat and entropy production in out of equilibrium systems. We will discuss the important difference between the applications of these concepts to stochastic systems and to a second class of systems (chaotic systems) where the fluctuations are induced either by chaotic flows or by fluctuating driving forces. We will mainly analyze the stochastic systems using the measurements performed in two experiments : a) a harmonic oscillator driven out of equilibrium by an external force b) a colloidal particle trapped in a time dependent double well potential. We will rapidly describe some consequences of fluctuation theorems and some useful applications to the analysis of experimental data. As an example the case of a molecular motor will be analyzed in some details. Finally we will discuss the problems related to the applications of fluctuation theorems to chaotic systems.

Contents

1 Introduction **2**

2 Work and heat fluctuations in the harmonic oscillator **3**
2.1 The experimental set-up . . . 4
2.2 The equation of motion . . . 4
2.2.1 *Equilibrium* . . . 5
2.3 Non-equilibrium Steady State (NESS): Sinusoidal forcing . . . 5
2.4 Energy balance . . . 6
2.5 Heat fluctuations . . . 7

3 Fluctuation theorem **8**
3.1 Short history of FTs . . . 9
3.2 FTs for Gaussian variables . . . 9
3.3 FTs for W_τ and Q_τ measured in the harmonic oscillator . . . 9
3.4 Comparison with theory . . . 11
3.5 The trajectory dependent entropy . . . 11

4 The non-linear case: stochastic resonance **14**

5 Applications of Fluctuation Theorems **16**
5.1 Measuring the power of a molecular motor 17

6 The chaotic systems **18**
6.1 Experimental test 19
6.1.1 *Granular media* 19
6.1.2 *Mechanical waves* 20

7 Summary and concluding remarks **21**

1 Introduction

This article is a review of the main experimental applications of Fluctuation Theorems (FTs) and summarizes the plenary talk given at STATPHYS24. In order to define the main contents let us consider several simple examples. The simplest and most basic out of equilibrium system is a thermal conductor whose extremities are connected to two heat baths at different temperatures, as sketched in fig.1. The second law of thermodynamics imposes that in average the heat flows from the hot to the cold reservoir (from H to C in fig.1). However the second law does not say anything about fluctuations and in principle one can observe for a short time a heat current in the opposite direction. What is the probability of observing these rare events ? As a general rule when the size of the system decreases the role of fluctuations increases. Thus from an experimental point of view it is reasonable to think that such rare events can be observed in systems that are small. A good candidate could be for example the thermal conduction in a nanotube whose extremities are connected to two heat baths [1], exactly in the spirit of fig.1. In reality in this kind of experiments the measure of the mean quantities [1] is already difficult and of course the analysis of fluctuations is even more complicated. However there is an electrical analogy, shown in fig.1b), of the thermal model of fig.1a). Let us consider an electrical conductor connected to a potential difference $V = V_A - V_B$ and kept at temperature T by a heat bath . If the mean current $\bar{I} = V/R$ (R being the electrical resistance of the conductor) is of the order of 10^{-13} A and the injected power is about $100 k_B T \simeq 10^{-19}$ J (k_B is the Boltzmann constant) then the instantaneous current inside the resistance has fluctuations whose amplitude is comparable to the mean, as shown in fig.1c). The variance of these fluctuations is $\delta I^2 \simeq k_B T/(R\,\tau_0)$ where τ_0 is the characteristic time constant of the electrical circuit. In the specific case of Fig. 1c) the current reverses with respect to the mean value. The probability of having those negative currents have been studied both theoretically and experimentally in ref. [2, 3] within the context of fluctuation theorems, that we will present in sec.3.

We discuss a second example where the source of fluctuation is not the coupling with a thermal bath, as in the case of the electrical conductor, but it is either a chaotic flows or a chaotic force produced by the non-linear interaction of many degrees of freedom of a dissipative system sustained by an external driving. We will refer to them as chaotic systems. Let us consider a turbulent wind flowing around an object as sketched in fig.2a),b). The wind exerts a mean force F_0 on the object but the instantaneous force, plotted in fig.2c), is a strongly fluctuating quantity which presents negative values [4], i.e. the object moves against the wind,fig.2b). In such a case the mean work done by the wind on the object is about $0.$ J$\simeq 10^{20} k_B T$ and obviously thermal fluctuations do not play any role but so does the chaotic flow, which produces the fluctuations. Other similar examples can be found for example in shaken granular media [5, 6], discussed in sec.6.

These examples stress that in the two experiments the electrical conductor and the turbulent wind we may observe the counterintuitive effect that the instantaneous response of the system is opposite to the mean value, in other words the system has an instantaneous negative entropy production rate. This effect is induced by the thermal fluctuations in the first case and by the chaotic flow in the second case. The question that we want analyze in this article is whether the Fluctuations Theorem (defined in section 3) is able to predict the probability of these rare events in both cases, i.e. for the stochastic and the chaotic systems. We will take an experimentalist approach and we will use experimental results in order to introduce the main concepts.

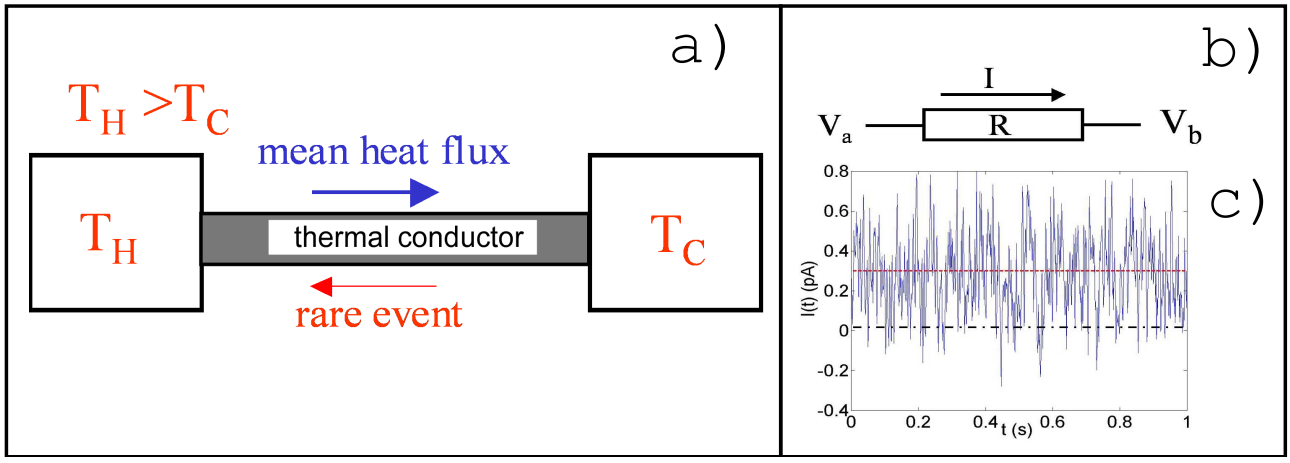

Figure 1: a) Schematic representation of a conductor whose extremities are in contact with two heat baths at temperature T_H and T_C with $T_H > T_C$. b) Electrical analogy. A conductor of electrical resistance R and kept at a temperature T is submitted to a potential difference $V = V_a - V_b$. c) Instantaneous current I flowing into the resistance using $R = 10$ MΩ, $T = 300$ K and $\tau_0 = 2$ ms.

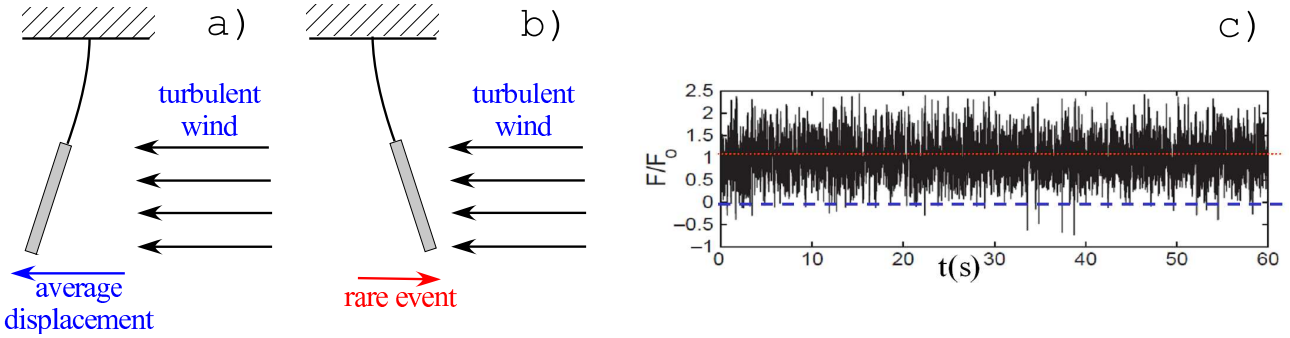

Figure 2: a)and b) Schematic representation of an object suspended by an elastic beam and submitted to the pressure of a turbulent wind a) average behavior b) rare event. c) Time evolution of the measured instantaneous force exerted by the turbulent wind on the object. The details of this experiment can be found [4]

The largest part of the article concerns stochastic systems described by a Langevin dynamics. For chaotic systems we will mainly discuss the difficulty of comparing the experimental results with the theoretical predictions. The article is organized as follows. In section 2 we present the experimental results on the energy fluctuations measured in a harmonic oscillator driven out of equilibrium by an external force. In section 3 the experimental results on the harmonic oscillator are used to introduce the property of Fluctuation Theorems (FTs). In section 4 the non linear case of a Brownian particle confined in a time dependent double well potential is presented. In section 5 we introduce the applications of the FT, and as a more specific example we describe the measure of the torque of a molecular motor. Finally in section 6 we discuss the chaotic systems and we conclude in section 7.

2 Work and heat fluctuations in the harmonic oscillator

The choice of discussing the dynamics of the harmonic oscillator is dictated by the fact that it is relevant for many practical applications such as the measure of the elasticity of nanotubes[7], the dynamics of the tip of an AFM [8], the MEMS and the thermal rheometer that we developed several years ago to study the rheology of complex fluids [9, 10].

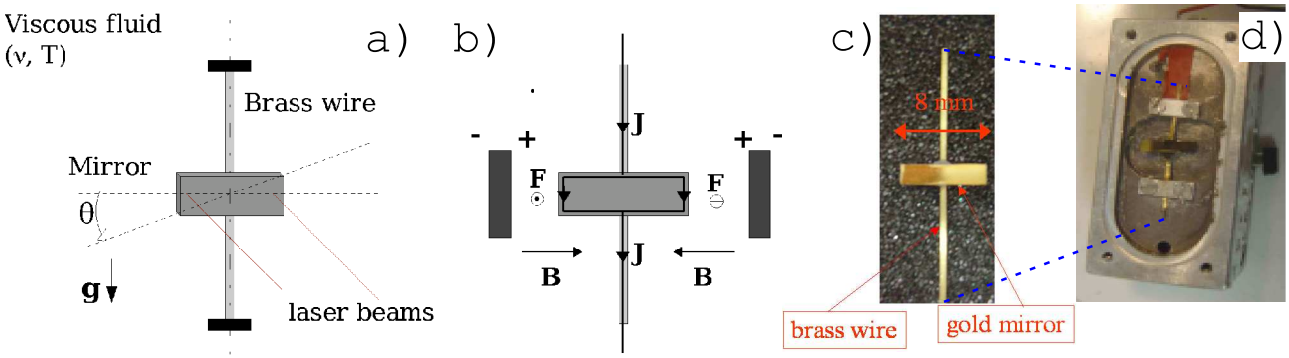

Figure 3: a) The torsion pendulum. b) The magnetostatic forcing. c) Picture of the pendulum. d) Cell where the pendulum is installed.

2.1 The experimental set-up

This device is a very sensitive torsion pendulum as sketched in fig.3a). It is composed by a brass wire (length 10 mm, width 0.5 mm, thickness 50 μm) and a glass mirror with a golden surface, fig.3c). The mirror (length 2 mm, width 8 mm, thickness 1 mm) is glued in the middle of the brass wire. The elastic torsional stiffness of the wire is $C = 4.65 \cdot 10^{-4}$ N.m.rad^{-1}. It is enclosed in a cell, fig.3d), which is filled by a fluid. We used either air or a water-glycerol mixture at 60% concentration. The system is a harmonic oscillator with resonant frequency $f_o = \sqrt{C/I_{\text{eff}}}/(2\pi) = \omega_0/(2\pi)$ and a relaxation time $\tau_\alpha = 2I_{\text{eff}}/\nu = 1/\alpha$. I_{eff} is the total moment of inertia of the displaced masses (*i.e.* the mirror and the mass of displaced fluid) [11]. The damping has two contributions : the viscous damping ν of the surrounding fluid and the viscoelasticity of the brass wire.

The angular displacement of the pendulum θ is measured by a differential interferometer [12, 13, 14, 15] which uses the two laser beams reflected by the mirror fig.3a). The measurement noise is two orders of magnitude smaller than thermal fluctuations of the pendulum. $\theta(t)$ is acquired with a resolution of 24 bits at a sampling rate of 8192 Hz, which is about 40 times f_o. We drive the system out-of-equilibrium by forcing it with an external torque M by means of a small electric current J flowing in a coil glued behind the mirror (Fig. 3b). The coil is inside a static magnetic field. The displacements of the coil and therefore the angular displacements of the mirror are much smaller than the spatial scale of inhomogeneity of the magnetic field. So the torque is proportional to the injected current : $M = A.J$; the slope A depends on the geometry of the system. The practical realization of the montage is shown in figs. 3c), 3d). In equilibrium the variance $\delta\theta^2$ of the thermal fluctuations of θ can be obtained from equipartition, i.e. $\delta\theta = \sqrt{k_B\, T/C} \simeq 2$ nrad for our pendulum, where T is the temperature of the surrounding fluid.

2.2 The equation of motion

The dynamics of the torsion pendulum can be assimilated to that of a harmonic oscillator damped by the viscoelasticity of the torsion wire and the viscosity of the surrounding fluid, whose equation of motion reads in the temporal domain

$$I_{\text{eff}}\,\ddot{\theta} + \int_{-\infty}^{t} G(t-t')\,\dot{\theta}(t')\mathrm{d}t' + C\theta = M + \eta, \tag{1}$$

where G is the memory kernel and η the thermal noise. In Fourier space (in the frequency range of our interest) this equation takes the simple form

$$[-I_{\text{eff}}\,\omega^2 + \hat{C}]\,\hat{\theta} = \hat{M} + \hat{\eta}, \tag{2}$$

where $\hat{\cdot}$ denotes the Fourier transform and $\hat{C} = C + i[C_1'' + \omega C_2'']$ is the complex frequency-dependent elastic stiffness of the system. C_1'' and C_2'' are the viscoelastic and viscous components of the damping term.

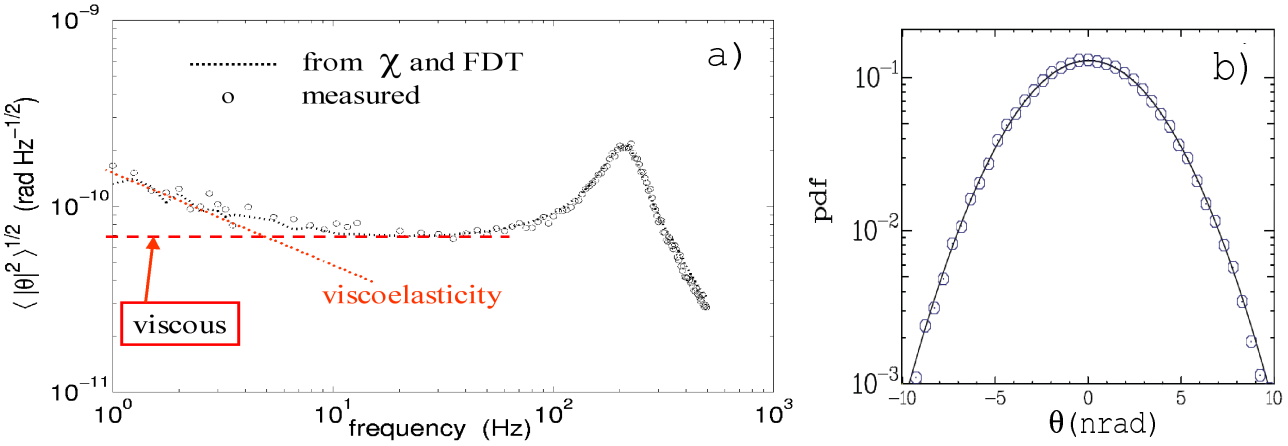

Figure 4: Equilibrium: The pendulum inside a glycerol-water mixture with $M = 0$. a) Square root of the power spectral density of θ. $\circ$ directly measured spectrum, black dotted line is the spectrum estimated from the measure of χ and using eq.3 The red dashed and dotted lines show the viscous and viscoelastic component of the damping respectively. b) Probability density function of θ. The continuous line is a Gaussian fit

2.2.1 *Equilibrium*

At equilibrium,*i.e.* $M = 0$, the Fluctuation Dissipation Theorem (FDT) gives a relation between the amplitude of the thermal angular fluctuations of the oscillator and its response function. The response function of the system $\hat{\chi} = \hat{\theta}/\hat{M} = \frac{\hat{\theta}}{A\hat{j}}$ can be measured by applying a torque with a white spectrum. When $M = 0$, the amplitude of the thermal vibrations of the oscillator is related to its response function via the fluctuation-dissipation theorem (FDT). Therefore, the thermal fluctuation power spectral density (psd) of the torsion pendulum reads for positive frequencies

$$\langle|\hat{\theta}|^2\rangle = \frac{4k_BT}{\omega}\,\mathrm{Im}\,\hat{\chi} = \frac{4k_BT}{\omega}\,\frac{C_1'' + \omega\,C_2''}{[-I_{\mathrm{eff}}\,\omega^2 + C]^2 + [C_1'' + \omega\,C_2'']^2}. \tag{3}$$

The brackets are ensemble averages. As an example, the spectrum of θ measured in the glycerol-water mixture is shown in fig.4a). In this case the resonance frequency is $f_o = \sqrt{C/I_{\mathrm{eff}}}/(2\pi) = \omega_0/(2\pi) = 217$ Hz and the relaxation time $\tau_\alpha = 2I_{\mathrm{eff}}/\nu = 1/\alpha = 9.5$ ms The measured spectrum is compared with that obtained from eq.3 using the measured χ. The viscoelastic component at low frequencies correspond to a constant $C_1'' \neq 0$. Indeed if $\omega \to 0$ then from eq.3 $\langle|\hat{\theta}|^2\rangle \propto 1/\omega$ as seen in fig.4a). Instead if $C_1'' = 0$ then for $\omega \to 0$ from eq.3 the spectrum is constant as a function of ω. It is important to stress that in the viscoelastic case the noise η is correlated and the process is not Markovian, whereas in the viscous case the process is Markovian. Thus by changing the quality of the fluid surrounding the pendulum one can tune the Markovian nature of the process. In the following we will consider only the experiment in the glycerol-water mixture where the viscoelastic contribution is visible only at very low frequencies and is therefore negligible. This allows a more precise comparison with theoretical predictions often obtained for Markovian processes. The probability density function (pdf) of θ, plotted in fig.4b), is a Gaussian.

2.3 Non-equilibrium Steady State (NESS): Sinusoidal forcing

We now consider a periodic forcing of amplitude M_o and frequency ω_d, i.e. $M(t) = M_o \sin(\omega_d t)$ [14]-[17]. This is a very common kind of forcing which has been already studied in the case of the first order Langevin equation [18] and of the two level system [19] and in a different context for the second order Langevin equation [20]. Furthermore this is a very general case because using Fourier transform, any periodical forcing can be decomposed in a sum of sinusoidal forcing. We explain here the behavior of a single mode. Experiments have been performed at various M_o and ω_d. We present here the results for a particular amplitude and frequency:

$M_o = 0.78$ pN.m and $\omega_d/(2\pi) = 64$ Hz. This torque is plotted in Fig. 5a. The mean of the response to this torque is sinusoidal, with the same frequency, as can be seen in Fig. 5b. The system is clearly in a non-equilibrium steady state (NESS).

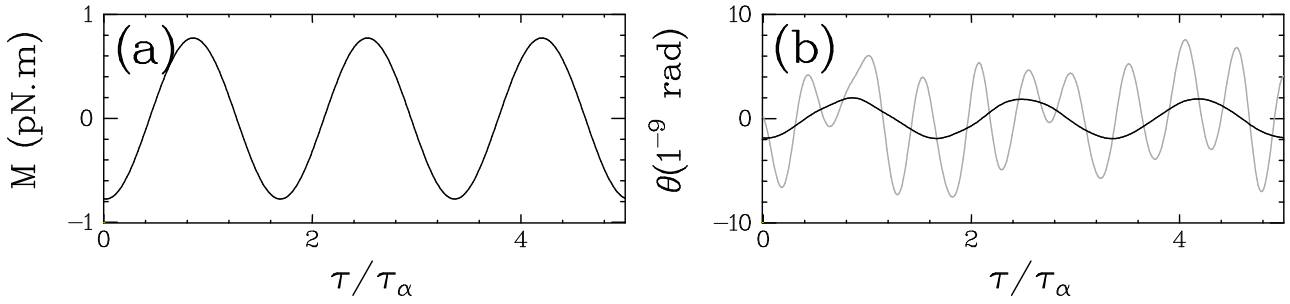

Figure 5: a) Sinusoidal driving torque applied to the oscillator. b) Response of the oscillator to this periodic forcing (gray line) ; the dark line represents the mean response $\langle\theta(t)\rangle$.

The work done by the torque $M(t)$ on a time $\tau_n = 2\pi\ n/\omega_d$ is

$$W_n = W_{\tau=\tau_n} = \int_{t_i}^{t_i+\tau_n} M(t)\frac{d\theta}{dt}dt \tag{4}$$

As θ fluctuates also W_n is a fluctuating quantity whose probability density function (pdf) is plotted in fig. 6a) for various n. This plot has interesting features. Specifically, work fluctuations are Gaussian for all values of n and W_τ takes negative values as long as τ_n is not too large. The probability of having negative values of W_τ decreases when τ_n is increased. There is a finite probability of having negative values of the work, in other words the system may have an instantaneous negative entropy production rate although the average of the work $< W_n >$ is of course positive ($< . >$ stands for ensemble average). In this specific example is $< W_n >= 0.04\ n(k_B\ T)$. We now consider the energy balance for the system.

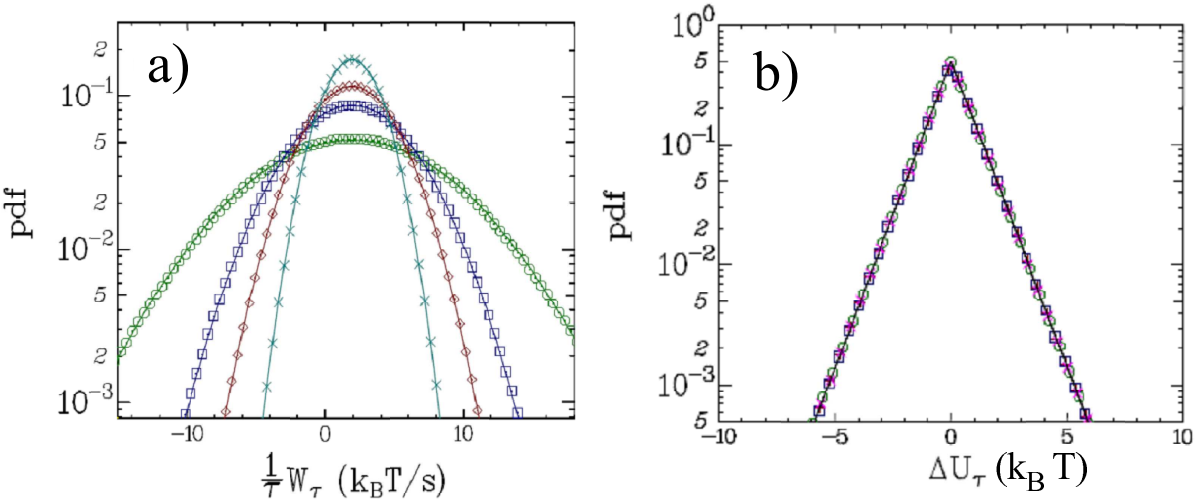

Figure 6: Sinusoidal forcing. a) Pdf of W_τ; $n = 7$ ($\circ$), $n = 15$ ($\square$), $n = 25$ ($\diamond$) and $n = 50$ ($\times$). b) Pdf of ΔU_τ

2.4 Energy balance

As the fluid is rather viscous we will take into account only the standard viscosity that is $C_1'' = 0$ and $C_2'' = \nu$. In such a case eq.1 simplifies

$$I_{\text{eff}}\,\frac{\mathrm{d}^2\theta}{\mathrm{d}t^2} + \nu\,\frac{\mathrm{d}\theta}{\mathrm{d}t} + C\,\theta = M + \eta, \tag{5}$$

where η is the thermal noise, which in this case is delta-correlated in time: $< \eta(t)\ \eta(t') >= 2\ k_B\ T\ \nu\delta(t-t')$.

When the system is driven out of equilibrium using a deterministic torque, it receives some work and a fraction of this energy is dissipated into the heat bath. Multiplying Eq. (5) by $\dot{\theta}$ and integrating between t_i and $t_i+\tau$, one obtains a formulation of the first law of thermodynamics between the two states at time t_i and $t_i+\tau$ (Eq. (6)). This formulation has been first proposed in ref.[21] and used in other theoretical and experimental works [22, 18]. The change in internal energy ΔU_τ of the oscillator over a time τ, starting at a time t_i, is written as:

$$\Delta U_\tau = U(t_i+\tau) - U(t_i) = W_\tau - Q_\tau \tag{6}$$

where W_τ is the work done on the system over a time τ :

$$W_\tau = \int_{t_i}^{t_i+\tau} M(t')\frac{\mathrm{d}\theta}{\mathrm{d}t}(t')\mathrm{d}t' \tag{7}$$

and Q_τ is the heat dissipated by the system. The internal energy is the sum of the potential energy and the kinetic energy :

$$U(t) = \left\{ \frac{1}{2} I_{\mathrm{eff}} \left[\frac{\mathrm{d}\theta}{\mathrm{d}t}(t)\right]^2 + \frac{1}{2} C\theta(t)^2 \right\}. \tag{8}$$

The heat transfer Q_τ is deduced from equation (6) ; it has two contributions :

$$\begin{aligned} Q_\tau &= W_\tau - \Delta U_\tau \\ &= \int_{t_i}^{t_i+\tau} \nu \left[\frac{\mathrm{d}\theta}{\mathrm{d}t}(t')\right]^2 \mathrm{d}t' - \int_{t_i}^{t_i+\tau} \eta(t')\frac{\mathrm{d}\theta}{\mathrm{d}t}(t')\mathrm{d}t'. \end{aligned} \tag{9}$$

The first term corresponds to the viscous dissipation and is always positive, whereas the second term can be interpreted as the work of the thermal noise which has a fluctuating sign. The second law of thermodynamics imposes $\langle Q_\tau \rangle$ to be positive.

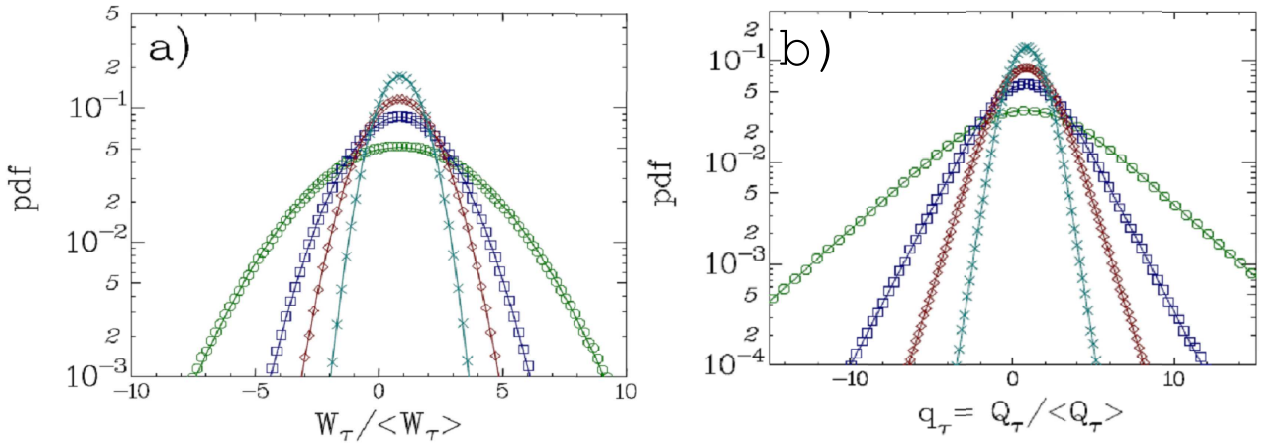

Figure 7: Sinusoidal forcing. a) Pdf of W_τ b) Pdf of Q_τ for various n: $n=7$ ($\circ$), $n=15$ ($\square$), $n=25$ ($\diamond$) and $n=50$ ($\times$). The continuous lines in this figures are not fits but are analytical predictions obtained from the Lnagevin dynamics as discussed in sect.3.4

2.5 Heat fluctuations

The dissipated heat Q_τ can not be directly measured because we have seen that eq.9 contains the work of the noise (the heat bath) that experimentally is impossible to measure, because η is unknown. However Q_τ can

be obtained indirectly from the measure of W_τ and ΔU_τ, whose pdf measured during the periodic forcing are exponential for any τ, as shown in fig.6b. We first do some comments on the average values. The average of ΔU_τ is obviously vanishing because the time τ is a multiple of the period of the forcing. Therefore $\langle W_n \rangle$ and $\langle Q_n \rangle$ are equal.

We rescale the work W_τ (the heat Q_τ) by the average work $\langle W_\tau \rangle$ (the average heat $\langle Q_\tau \rangle$) and define: $w_\tau = \frac{W_\tau}{\langle W_\tau \rangle}$ ($q_\tau = \frac{Q_\tau}{\langle Q_\tau \rangle}$). In the present article, x_τ, respectively X_τ, stands for either w_τ or q_τ, respectively W_τ or Q_τ.

We compare now the pdf of w_τ and q_τ in Fig. 7. The pdfs of heat fluctuations q_n have exponential tails (Fig. 7b). It is interesting to stress that although the two variables W_τ and Q_τ have the same mean values they have a very different pdf. The pdf of w_τ are gaussian whereas those of q_τ are exponential. On a first approximation the pdf of q_τ are the convolution of a Gaussian (the pdf of W_τ) and exponential (the pdf of ΔU_τ). In Figs. 7 the continuous lines are analytical predictions obtained from the Langevin dynamics with no adjustable parameter (see sect.3.4).

3 Fluctuation theorem

In the previous section we have seen that both W_τ and Q_τ present negative values, *i.e.* the second law is verified only on average but the entropy production can have instantaneously negative values. The probabilities of getting positive and negative entropy production are quantitatively related in non-equilibrium systems by the Fluctuation Theorem (FTs).

There are two classes of FTs. The *Stationary State Fluctuation Theorem* (SSFT) considers a non-equilibrium steady state. The *Transient Fluctuation Theorem* (TFT) describes transient non-equilibrium states where τ measures the time since the system left the equilibrium state. A Fluctuation Relation (FR) examines the symmetry around 0 of the probability density function (pdf) $p(x_\tau)$ of a quantity x_τ, as defined in the previous section. It compares the probability to have a positive event ($x_\tau = +x$) versus the probability to have a negative event ($x_\tau = -x$). We quantify the FT using a function S (symmetry function) :

$$S(x_\tau) = \frac{k_B\, T}{\langle X_\tau \rangle} \ln \left(\frac{p(x_\tau = +x)}{p(x_\tau = -x)} \right). \tag{10}$$

The *Transient Fluctuation Theorem* (TFT) states that the symmetry function is linear with x_τ for any values of the time integration τ and the proportionality coefficient is equal to 1 for any value of τ.

$$S(x_\tau) = x_\tau, \quad \forall x_\tau, \quad \forall \tau. \tag{11}$$

Contrary to TFT, the *Stationary State Fluctuation Theorem* (SSFT) holds only in the limit of infinite time (τ).

$$\lim_{\tau \to \infty} S(x_\tau) = x_\tau. \tag{12}$$

In the following we will assume linearity at finite time τ [2, 29] and use the following general expression :

$$S(x_\tau) = \Sigma_x(\tau)\, x_\tau \tag{13}$$

where for SSFT $\Sigma_x(\tau)$ takes into account the finite time corrections and $\lim_{\tau \to \infty} \Sigma_x(\tau) = 1$ whereas $\Sigma_x(\tau) = 1, \quad \forall\, \tau$ for TFT.

However these claims are not universal because they depend on the kind of x_τ which is used. Specifically we will see in the next sections that the results are not exactly the same if X_τ is replaced by any one of W_τ, Q_τ and $(T\ s_{tot,\tau})$, defined in sect.3.3. Furthermore the definitions given in this section are appropriate for stochastic systems and in sect.6 we will discuss the differences between stochastic and chaotic systems.

3.1 Short history of FTs

The first numerical evidence of relations of this kind has been given by Evans et al. in ref.[23] whereas the TFT was proved in ref.[24]. In 1995 Gallavotti and Cohen [25] proved SSFT for dynamical systems although in such a case x_τ takes a different meaning that we will discuss in sect.6. The proof of SSFT has been extended to stochastic dynamics in ref. [2, 26, 27, 28, 29]. Furthermore van Zon and Cohen proved that there is an important difference between the FTs for the injected power and those for the dissipated power [2, 29]. The SSFT has been proved also for other quantities such as the dissipation function [30] and the total entropy [31, 32]. Other theoretical papers studied FT and the reader may find a review in ref.[33, 34]. Experiments searching for FTs have been performed in dynamical systems [4, 5, 36], but interpretations are very difficult because a quantitative comparison with theoretical prediction can be doubtful. Other experiments have been performed in stochastic systems described by a first order Langevin equation: a Brownian particle in a moving optical trap [37] and an out-of-equilibrium electrical circuit [3] in which existing theoretical predictions [2, 29] were verified. Other experimental tests for FTs have been performed on driven two level systems [19] and on colloids [18].

3.2 FTs for Gaussian variables

Let us suppose the the variable X_τ has a Gaussian distribution of mean $< X_\tau >$ and variance $\sigma^2_{X_\tau}$. It is easy to show that in order to satisfy FTs, the variable X_τ must have the following statistical property:

$$\sigma^2_{X_\tau} = 2\, k_B\, T\ < X_\tau > \tag{14}$$

This is an interesting relation because it imposes that the relative fluctuations of X_τ are

$$\frac{\sigma_{X_\tau}}{X_\tau} = \sqrt{\frac{2\, k_B\, T}{< X_\tau >}} \tag{15}$$

This means that the probability of having negative events reduces by increasing X_τ, specifically from eq.15 it follows that $P(X_\tau < 0) = \mathrm{erfc}(\sqrt{< \mathrm{X}_\tau > /(2\ \mathrm{k_B T})})$ where erfc is the complementary error function. It is now possible to estimate the length of the time interval t_{obs} needed to observe at least one negative event, which is:

$$t_{obs} = \frac{\tau}{\mathrm{erfc}\left(\sqrt{\frac{<\mathrm{X}_\tau>}{2\ \mathrm{k_B\ T}}}\right)} \tag{16}$$

where we used the fact that all the values W_τ computed on different intervals of length τ are independent, which is certainly true if τ is larger than the correlation time.

Let us consider the specific example of section 2.3, i.e. $< W_\tau >= 0.04 n(k_B T)$ at $\omega_d/(2\ \pi) = 67$ Hz, $M_o = 0.78$ pN.m and $\tau = 2\pi n/\omega_d$. The pdf of W_τ are Gaussian in this case (Fig.6) and, as we will see in the next section, they satisfy SSFT for large τ. Therefore eq.15 holds for $X_\tau = W_\tau$ and we may estimate t_{obs} in the asymptotic limit $\tau_\alpha << \tau$. For example at $n = 200$, one obtains from the above mentioned experimental values $\tau \simeq 3s >> \tau_\alpha$ and $< W_\tau >= 8 k_B T$. Inserting these experimental values in eq.15 one gets roughly a negative event over an observational time $t_{obs} \simeq 641s$, which is already a rather long time for the distance between two events. For larger n and larger M_0 this time becomes exponentially large. This justifies the fact that millions of data are necessary in order to have a reliable measure of SSFT.

3.3 FTs for W_τ and Q_τ measured in the harmonic oscillator

The questions we ask are whether for finite time FTs are satisfied for either $x_\tau = w_\tau$ or $x_\tau = q_\tau$ and what are the finite time corrections. In a first time, we test the correction to the proportionality between the symmetry function $S(x_\tau)$ and x_τ. In the region where the symmetry function is linear with x_τ, we define the slope $\Sigma_x(\tau)$, i.e. $S(x_\tau) = \Sigma_x(\tau) x_\tau$. In a second time we measure finite time corrections to the value $\Sigma_x(\tau) = 1$ which is the asymptotic value expected from FTs.

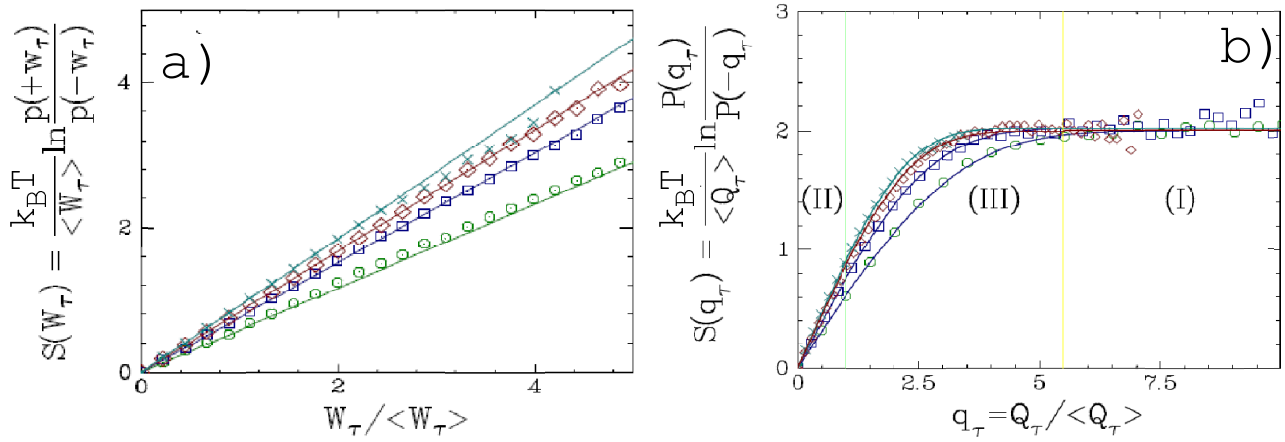

Figure 8: Sinusoidal forcing. Symmetry functions for SSFT. a) Symmetry functions $S(w_\tau)$ plotted as a function of w_τ for various n: $n = 7$ ($\circ$), $n = 15$ ($\Box$), $n = 25$ ($\diamond$) and $n = 50$ ($\times$). For all n the dependence of $S(w_\tau)$ on w_τ is linear, with slope $\Sigma_w(\tau)$. b) Symmetry functions $S(q_\tau)$ plotted as a function of q_τ for various n. The dependence of $S(q_\tau)$ on q_τ is linear only for $q_\tau < 1$. Continuous lines are is theoretical predictions.

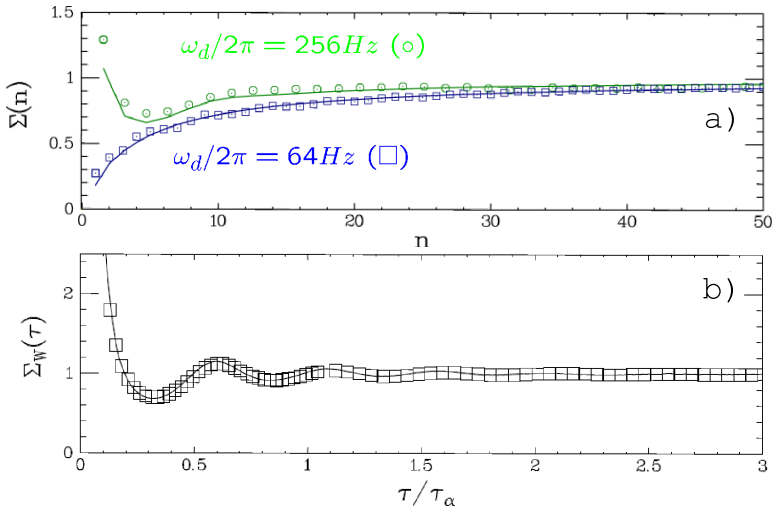

Figure 9: Finite time corrections for SSFT. a) Sinusoidal forcing. $\Sigma_w(\tau)$ as a function of n obtained from the slopes of the straight lines of Fig.8a) ($\Box$). The circles correspond to another measurement performed at a different frequency. The finite time corrections depend on the driving frequency. The slope $\Sigma_q(\tau)$ measured for $q_\tau < 1$ (Fig.8b) have exactly the same values of $S_w(\tau)$ as a function of n. b) Linear forcing. $\Sigma_w(\tau)$ measured as a function of τ with the driving torque M has a linear dependence on time. The finite time corrections depend on form of the driving.

In this review article we will focus on the SSFT applied to the experimental results of sect. 2.3 and to other examples. The TFT will be not discussed here and the interested readers may look at ref.[17].

From the pdfs of w_τ and q_τ plotted in Figs.7, we compute the symmetry functions defined in eq.10. The symmetry function $S(w_n)$ are plotted in Fig. 8a) as a function of w_n. They are linear in w_n. The slope $\Sigma_w(n)$ is not equal to 1 for all n but there is a correction at finite time (Fig. 9a). Nevertheless, $\Sigma_w(n)$ tends to 1 for large n. Thus SSFT is satisfied for W_τ and for a sinusoidal forcing. The convergence is very slow and we have to wait a large number of periods of forcing for the slope to be 1 (after 30 periods, the slope is still 0.9). This behavior is independent of the amplitude of the forcing M_o and consequently of the mean value of the work $\langle W_n\rangle$, which, as explained in sec.3.2, changes only the time needed to observe a negative event. The system

satisfies the SSFT for all forcing frequencies ω_d but finite time corrections depend on ω_d, as can be seen in Fig. 9a).

We now analyze the pdf of q_τ (Fig.7b)) and we compute the symmetry functions $S(q_n)$ of q_n plotted in Fig. 8b) for different values of n. They are clearly very different from those of w_n plotted in Fig. 8a). For $S(q_n)$ three different regions appear:

(I) For large fluctuations q_n, $S(q_n)$ equals 2. When τ tends to infinity, this region spans from $q_n = 3$ to infinity.

(II) For small fluctuations q_n, $S(q_n)$ is a linear function of q_n. We then define $\Sigma_q(n)$ as the slope of the function $S(q_n)$, *i.e.* $S(q_n) = \Sigma_q(n)\, q_n$. We have measured [17] that $\Sigma_q(n) = \Sigma_w(n)$ for all the values of n, i.e. finite time corrections are the same for heat and work. Thus $\Sigma_q(n)$ tends to 1 when τ is increased and SSFT holds in this region II which spans from $q_n = 0$ up to $q_n = 1$ for large τ. This effect has been discussed for the first time in refs.[29, 2].

(III) A smooth connection between the two behaviors.

These regions define the Fluctuation Relation from the heat dissipated by the oscillator. The limit for large τ of the symmetry function $S(q_\tau)$ is rather delicate and it has been discussed in ref.[17].

The conclusions of this experimental analysis is that SSFT holds for work for any value of w_τ whereas for heat it holds only for $q_\tau < 1$. The finite time correction to FTs, described by $1 - \Sigma$ are not universal. They are the same both for w_τ and q_τ but they depend on the driving frequency as shown in Fig.9a). Furthermore they depend on the kind of driving force. In Fig. 9b) we plot $\Sigma_w(\tau)$ measured when the harmonic oscillator is driven out of equilibrium by a linear ramp[1]. The difference with respect Fig. 9a) is quite evident.

3.4 Comparison with theory

This experimental analysis allows a very precise comparison with theoretical predictions using the Langevin equation (eq.5) and using two experimental observations: a) the properties of heat bath are not modified by the driving and b) the fluctuations of the W_τ are Gaussian (see also [38], where it is shown that in Langevin dynamics W_τ has a Gaussian distribution for any kind of deterministic driving force if the properties of the bath are not modified by the driving and the potential is harmonic). The observation in point a) is extremely important because it is always assumed to be true in all the theoretical analysis. In ref.[17] this point has been precisely checked. Using these experimental observations one can compute the pdf of q_τ and the finite time corrections $\Sigma(\tau)$ to SSFT (see ref.[17]). The continuous lines in Fig. 9, Fig. 8 and Fig. 6 are not fit but analytical predictions, with no adjustable parameters, derived from the Langevin dynamics of eq.5 (see ref.[17] for more details).

3.5 The trajectory dependent entropy

In previous sections we have studied the energy W_τ injected into the system in the time τ and the energy dissipated towards the heat bath Q_τ. These two quantities and the internal energy are related by the first law of thermodynamics (eq.9). Following notations of ref [31], we define the entropy variation in the system during a time τ as :

$$\Delta s_{\mathrm{m},\tau} = \frac{1}{T} Q_\tau. \tag{17}$$

For thermostated systems, entropy change in medium behaves like the dissipated heat. The non-equilibrium Gibbs entropy is :

$$\langle s(t) \rangle = -k_B \int \mathrm{d}\vec{x} p(\vec{x}(t), t, \lambda_t) \ln p(\vec{x}(t), t, \lambda_t) \tag{18}$$

where λ_t denotes the set of control parameters at time t and $p(\vec{x}(t), t, \lambda_t)$ is the probability density function to find the particle at a position $\vec{x}(t)$ at time t, for the state corresponding to λ_t. This expression allows the

[1]The stationarity in the case of a ramp is discussed in ref.[29, 17]

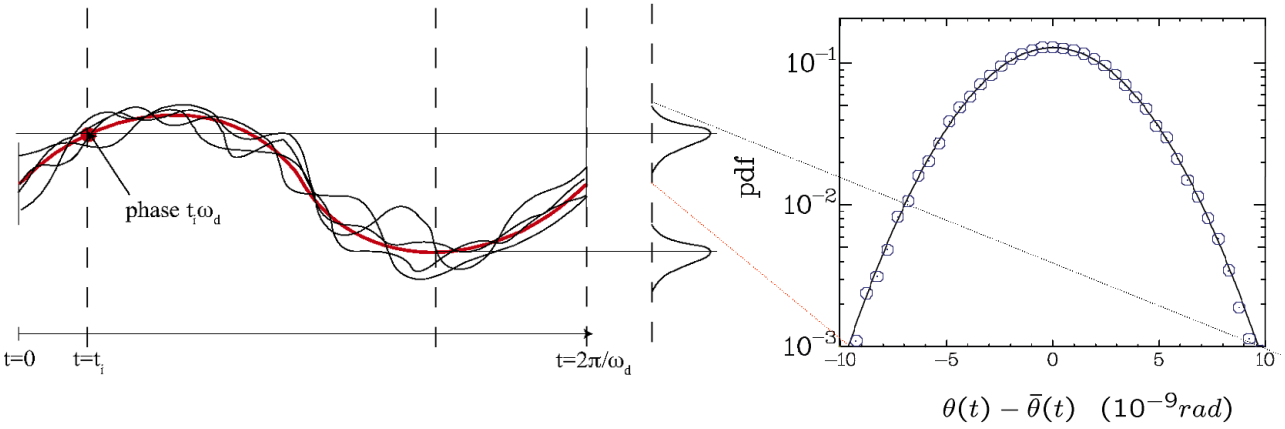

Figure 10: a) Schematic diagram illustrating the method to compute the trajectory dependent entropy, b) Pdf of $\theta(t)$ around the mean trajectory $< \theta(t) >$. The continuous line is the equilibrium distribution

definition of a "trajectory-dependent" entropy :

$$s(t) \equiv -k_B \ln p(\vec{x}(t), t, \lambda_t) \tag{19}$$

The variation $\Delta s_{\mathrm{tot},\tau}$ of the total entropy s_{tot} during a time τ is the sum of the entropy change in the system during τ and the variation of the "trajectory-dependent" entropy in a time τ, $\Delta s_\tau \equiv s(t+\tau) - s(t)$:

$$\Delta s_{\mathrm{tot},\tau} \equiv s_{\mathrm{tot}}(t+\tau) - s_{\mathrm{tot}}(t) = \Delta s_{\mathrm{m},\tau} + \Delta s_\tau \tag{20}$$

In this section, we study fluctuations of $\Delta s_{\mathrm{tot},\tau}$ computed using (17) and (19). We will show that $\Delta s_{\mathrm{tot},\tau}$ satisfies a SSFT for all τ. In ref. [32], the relevance of boundary terms like Δs_τ has been pointed out for Markovian processes.

We investigate the data of the harmonic oscillator described in sect.2.3.The probability to compute is the joint probability $p(\theta(t_i+\tau_n), \dot{\theta}(t_i+\tau_n), \varphi)$, where φ is the starting phase $\varphi = t_i\omega_d$. The system is linear, so $\theta(t_i+\tau_n), \dot{\theta}(t_i+\tau_n)$ are independent; thus the joint probability can be factorized into a product. The expression of the trajectory dependent entropy is :

$$\Delta s_{\tau_n} = -k_B \ln \left(\frac{p(\theta(t_i+\tau_n), \varphi)\ p(\dot{\theta}(t_i+\tau_n, \varphi))}{p(\theta(t_i+\tau_n), \varphi)\ p(\dot{\theta}(t_i+\tau_n, \varphi)} \right) \tag{21}$$

For computing correctly the trajectory dependent entropy, we have to calculate the $p(\theta(t_i), \varphi)$ and $p(\dot{\theta}(t_i), \varphi)$ for each initial phase φ (see Fig.10a). These distributions turn out to be independent of φ and they correspond to the equilibrium fluctuations of θ and $\dot{\theta}$ around the mean trajectory defined by $\langle\theta(t)\rangle$ and $\langle\dot{\theta}(t)\rangle$. The distribution of $\theta(t_i)$ is plotted in Fig.10b), where the continuous line corresponds to the equilibrium distribution. Once the $p(\theta(t_i, \varphi)$ and $p(\dot{\theta}(t_i), \varphi)$ are determined we compute the "trajectory-dependent" entropy. As fluctuations of θ and $\dot{\theta}$ are independent of φ we can average Δs_{τ_n} over φ which improves a lot the statistical accuracy. We stress that it is not equivalent to calculate first the pdfs over all values of φ — which would correspond here to the convolution of the pdf of the fluctuations with the pdf of a periodic signal — and then compute the trajectory dependent entropy. The results are shown in Fig. 11.

In Fig. 11a), we recall the main results for the dissipated heat $Q_\tau = T\Delta s_{\mathrm{m},\tau_n}$. Its average value $\langle T.\Delta s_{\mathrm{m},\tau_n}\rangle$ is linear in τ_n and equal to the injected work. The pdfs of $T.\Delta s_{\mathrm{m},\tau_n}$ are not Gaussian and extreme events have an exponential distribution. The pdf of the "trajectory-dependent" entropy is plotted in fig. 11b); it is exponential and independent of n. We superpose to it the pdf of the variation of internal energy divided by T at equilibrium: the two curves match perfectly within experimental errors, so the "trajectory-dependent" entropy can be considered as the entropy exchanged with the thermostat if the system is at equilibrium. The average

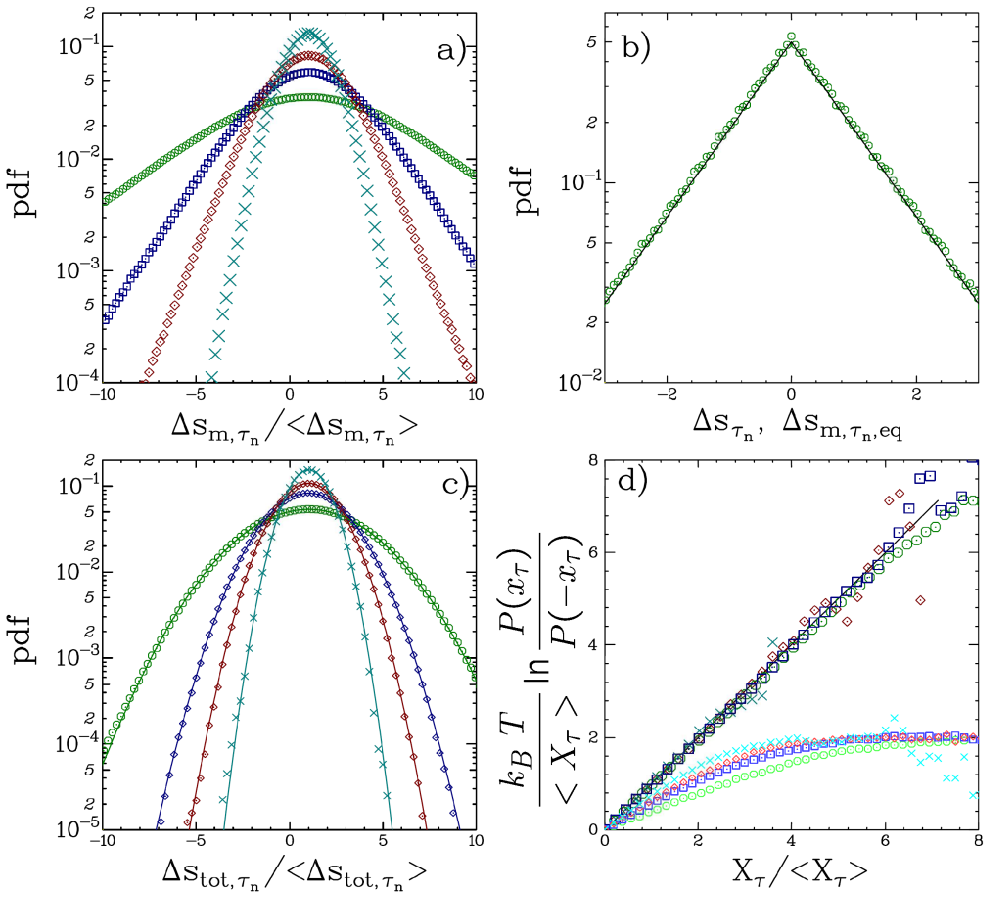

Figure 11: Torsion pendulum. a) pdfs of the normalized entropy variation $\Delta s_{\mathrm{m},\tau_\mathrm{n}}/\langle\Delta s_{\mathrm{m},\tau_\mathrm{n}}\rangle$ integrated over n periods of forcing, with $n = 7$ ($\circ$), $n = 15$ ($\square$), $n = 25$ ($\diamond$) and $n = 50$ ($\times$). b) pdfs of Δs_{τ_n}, the distribution is independent of n and here $n = 7$. Continuous line is the theoretical prediction for equilibrium entropy exchanged with thermal bath $\Delta s_{\mathrm{m},\tau_\mathrm{n},\mathrm{eq}}$. c) pdfs of the normalized total entropy $\Delta s_{\mathrm{tot},\tau_\mathrm{n}}/\langle\Delta s_{\mathrm{tot},\tau_\mathrm{n}}\rangle$, with $n = 7$ ($\circ$), $n = 15$ ($\square$), $n = 25$ ($\diamond$) and $n = 50$ ($\times$). d) Symmetry functions for the normalized entropy variation in the system (small symbols in light colors and X_τ stands for $T\,\Delta s_{\mathrm{m},\tau_\mathrm{n}} = Q_\tau$) and for the normalized total entropy (large symbols in dark colors and X_τ stands for $T\,\Delta s_{\mathrm{tot},\tau_\mathrm{n}}$) for the same values of n.

value of Δs_{τ_n} is zero, so the average value of the total entropy is equal to the average of injected power divided by T. In Fig. 11c), we plot the pdfs of the normalized total entropy for four typical values of integration time. We find that the pdfs are Gaussian for any time.

The symmetry functions (eq.10) of the dissipated heat $S(T\Delta s_{\mathrm{m},\tau_\mathrm{n}} = Q_\tau)$ and the total entropy $S(T\Delta s_{\mathrm{tot},\tau_\mathrm{n}})$ are plotted in Fig. 11d). As we have already seen in Fig.8, $S(Q_\tau)$ is a non linear function of $Q_\tau = T\,\Delta s_{\mathrm{m},\tau}$. The linear behavior, with a slope that tends to 1 for large time, is observed only for for $\Delta s_{\mathrm{m},\tau_\mathrm{n}} < \langle\Delta s_{\mathrm{m},\tau_\mathrm{n}}\rangle < 1$. For the normalized total entropy, the symmetry functions are linear with $\Delta s_{\mathrm{tot},\tau_\mathrm{n}}$ for all values of $\Delta s_{\mathrm{tot},\tau_\mathrm{n}}$ and the slope is equal to 1 for all values of τ_n. Note that it is not exactly the case for the first values of τ_n because these are the times over which the statistical errors are the largest and the error in the slope is large.

For the harmonic oscillator we have obtained that the "trajectory-dependent" entropy can be considered as the entropy variation in the system in a time τ that one would have if the system was at equilibrium. Therefore the total entropy is the additional entropy due to the presence of the external forcing : *this is the part of entropy which is created by the non-equilibrium stationary process*. The total entropy (or excess entropy) satisfies the Fluctuation Theorem for all times and for all kinds of stationary external torque[31, 32]. More details on this

problem can be found in ref.[39].

4 The non-linear case: stochastic resonance

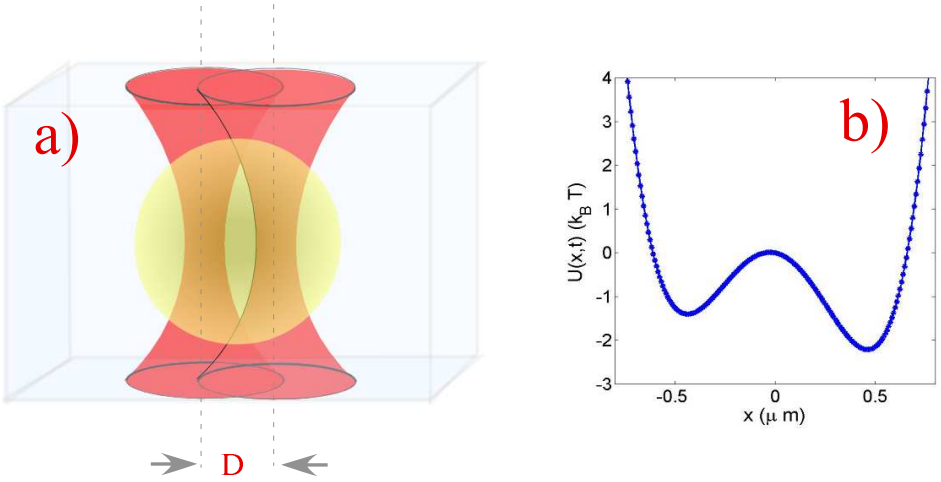

Figure 12: a) Drawing of the polystyrene particle trapped by two laser beams whose axis distance is about the radius of the bead. b) Potential felt by the bead trapped by the two laser beams. The barrier height between the two wells is about $2k_BT$.

The harmonic oscillator cannot be driven to a non linear regime without forcing it to such a high level where thermal fluctuations become negligible. Thus in order to study the non linear effects we change experiment and we measure the fluctuations of a Brownian particle trapped in a non-linear potential produced by two laser beams, as shown in Fig.12. It is very well known that a particle of small radius $R \simeq 2$ μm is trapped in the focus of a strongly focused laser beam, which produces a harmonic potential for the particle, whose Brownian motion is confined inside this potential well. When two laser beams are focused at a distance $D \simeq R$, as shown in Fig.12a) the particle has two equilibrium positions, i.e. the foci of the two beams. Thermal fluctuations may force the particle to move from one to the other. The particle feels an equilibrium potential $U_0(x) = ax^4 - bx^2 - dx$, shown in Fig.12b), where a, b and d are determined by the laser intensity and by the distance of the two focal points. This potential has been computed from the measured equilibrium distribution of the particle $P(x) \propto \exp(U_0(x))$. The right left asymmetry of the potential (Fig.12b) is induced by small unavoidable asymmetries, induced by the optics focusing the two laser beams. In our experiment the distance between the two spots is 1.45 μm, which produces a trap whose minima are at $x_{min} = \pm 0.45$ μm. The total intensity of the laser is 29 mW on the focal plane which corresponds to an inter-well barrier energy $\delta U_o = 1.8\ k_BT$, $ax_{min}^4 = 1.8\ k_BT$, $bx_{min}^2 = 3.6\ k_BT$ and $d|x_{min}| = 0.44\ k_BT$ (see ref.[40] for more experimental details). The rate at which the particle jumps from one potentials well to the other is determined by the Kramer's rate $r_k = \frac{1}{\tau_o}\exp(\frac{-\delta U_o}{k_B\ T})$ where τ_o is a characteristic time. In our experiment $r_k \simeq 0.3$ Hz at 300 K.

To drive the system out of equilibrium we periodically modulate the intensity of the two beams at low frequency. Thus the potential felt by the bead is the following profile:

$$U(x,t) = U_0(x) + U_p(x,t) = U_0 + c\,x\ \sin(2\pi f t), \tag{22}$$

with $c|x_{min}| = 0.81\ k_BT$. The amplitude of the time dependent perturbation is synchronously acquired with the bead trajectory.[2]

[2]The parameters given here are average parameters since the coefficients a, b and c, obtained from fitted steady distributions at given phases, vary with the phase ($\delta a/a \approx 10\%$, $\delta b/b \approx \delta c/c \approx 5\%$).

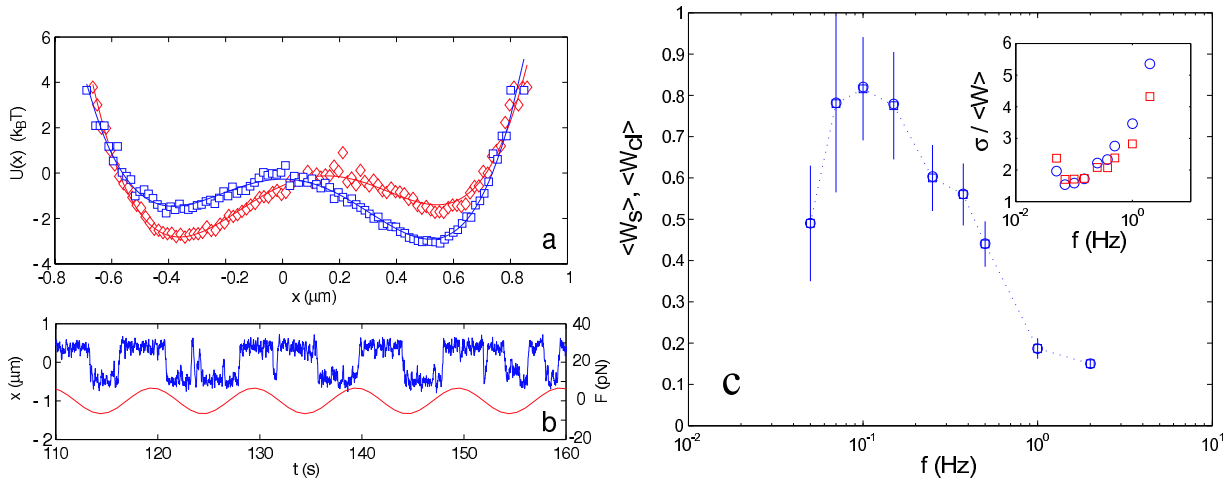

Figure 13: a) The perturbed potential at $t = \frac{1}{4f}$ and $t = \frac{3}{4f}$. b) Example of trajectory of the glass bead and the corresponding perturbation at $f = 0.1$ Hz. c) Mean injected energy in the system over a single period as a function of the driving frequency.$< W_s >$ $\square$ and $< W_{cl} >$ $\circ$ coincide as their mean values are equal within experimental errors. The error bars are computed from the standard deviation of the mean over different runs. Inset: Standard deviations of work distributions over a single period normalized by the average work as a function of the frequency (same symbols).

An example of the measured potential for $t = \frac{1}{4f}$ and $\frac{3}{4f}$ is shown on the Fig. 13a). This figure is obtained by measuring the probability distribution function $P(x,t)$ of x for fixed values of $c\sin(2\pi ft)$, it follows that $U(x,t) = -\ln(P(x,t))$.

The x position of the particle can be described by a Langevin equation:

$$\gamma\dot{x} = -\frac{\partial U(x,t)}{\partial x} + \eta, \tag{23}$$

with $\gamma = 1.61\ 10^{-8}$ N s m^{-1} the friction coefficient and η the thermal noise delta correlated in in time. When $c \neq 0$ the particle can experience a stochastic resonance [41], when the forcing frequency is close to the Kramer's rate. An example of the sinusoidal force with the corresponding position are shown on the figure 13b). Since the synchronization is not perfect, sometimes the particle receives energy from the perturbation, sometimes the bead moves against the perturbation leading to a negative work on the system. Two kinds of work can be defined in this experiments [40]

$$W_{s,n}(t) = \int_t^{t+t_f} dt \frac{\partial U(x,t)}{\partial t} \tag{24}$$

$$W_{cl,n}(t) = -\int_t^{t+t_f} dt\dot{x} \frac{\partial U_p(x,t)}{\partial x} \tag{25}$$

$$\tag{26}$$

where in this case $t_f = \frac{n}{f}$ is a multiple of the forcing period. The work $W_{s,n}$ is the stochastic work (used in Jarzynsky and Crooks relations [47, 49, 13]) and $W_{cl,n}$ is the classical work that will be discussed in this article. The results on $W_{s,n}$ are quite similar but there are subtle differences discussed in ref.[40].

We first measure the average work received over one period for different frequencies ($t_f = \frac{1}{f}$ in eq. 25). Each trajectory is here recorded during 3200 s in different consecutive runs, which corresponds to 160 up to 6400 forcing periods, for the range of frequencies explored. In order to increase the statistics we consider 10^5 different t_o. The figure 13c) shows the evolution of the mean work per period for both definitions of the

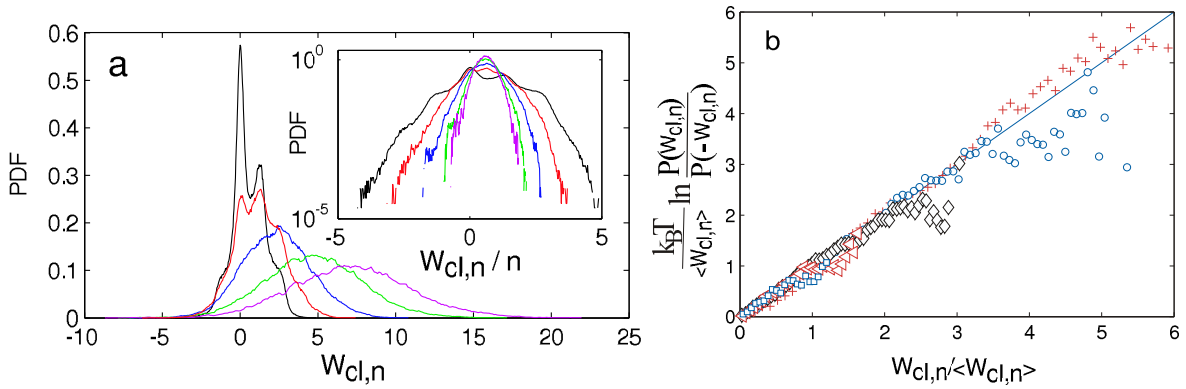

Figure 14: a) Distribution of classical work W_{cl} for different numbers of period $n = 1$, 2, 4, 8 and 12 ($f = 0.25$ Hz). Inset: Same data in lin-log. b) Normalized symmetry function as function of the normalized work for $n = 1$ (+), 2 ($\circ$), 4 ($\diamond$), 8 ($\triangle$), 12 ($\square$).

work. First, the input average work decreases to zero when the frequency tends to zero. Indeed, the bead hops randomly several times between the two wells during the period. Second, in the limit of high frequencies, the particle has not the time to jump on the other side of the trap but rather stays in the same well during the period, thus the input energy is again decreasing when increasing frequency. In the intermediate regime, the particle can almost synchronize with the periodical force and follows the evolution of the potential. The maximum of injected work is found around the frequency $f \approx 0.1$ Hz, which is comparable with half of the Kramers' rate of the fixed potential $r_K = 0.3$ Hz. This maximum of transferred energy shows that the stochastic resonance for a Brownian particle is a bona fide resonance, as it was previously shown in experiments using resident time distributions [42, 43] or directly in simulations [44, 45]. In the inset of Fig. 13, we plot the normalized standard deviation of work distributions ($\sigma / \langle W \rangle$) as a function of the forcing frequency. The curves present a minimum at the same frequency of 0.1 Hz, in agreement again with the resonance phenomena.

In order to study FT for stochastic resonance we choose for the external driving a frequency $f = 0.25$ Hz, which ensures a good statistic, by allowing the observation of the system over a sufficient number of periods. We compute the works and the dissipation using $1.5\ 10^6$ different t on time series which spans about 7500 period of the driving.

We consider the pdf $P(W_{cl})$ which is plotted in (Fig. 14a). Notice that for small n the distributions are double peaked and very complex. They tend to a gaussian for large n (inset of Fig. 14a). On Fig. 14b), we plot the normalized symmetry function of $W_{cl,n}$. We can see that the curves are close to the line of slope one. For high values of work, the dispersion of the data increases due to the lack of events. The slope tends toward 1 as expected by the SSFT. It is remarkable that straight lines are obtained even for n close to 1, where the distribution presents a very complex and unusual shape (Fig. 14a). We do not discuss here the case of $W_{s,n}$ as the behavior is quite similar to that of $W_{cl,n}$ [40]. The very fast convergency to the asymptotic value of the the SSFT is quite striking in this example. The measurement are in fully agreement with a realistic model based on the Fokker Planck equations where the measured values of $U(x,t)$ has been inserted [46]. This example shows the application of FT in a non-linear case where the distributions are strongly non-Gaussian.

5 Applications of Fluctuation Theorems

The Fluctuations Theorems have several important consequences such as the Jarzinsky and Crooks equalities[47, 48, 49], which are useful to compute the free energy difference between two equilibrium states using any kind of transformation[13, 15, 51, 50]. The Hatano-Sasa[22] relations and the recently derived Fluctaution Dissipation Theorems[52] are related to FTs and are useful to compute the response of a NESS using the steady state fluctuations of the NESS. As we have seen the FT allows the calculation of tiny amount heat, which can be

useful in many applications in aging systems [53, 54] and biological systems.

The FTs for Langevin systems can be used to measure an unknown averaged power. This idea has been discussed first in the context of electrical circuits [3] and in ref.[57] it has been applied for the first time to the measure of the the torque of a molecular motor. We discuss the method in some details in the next subsection.

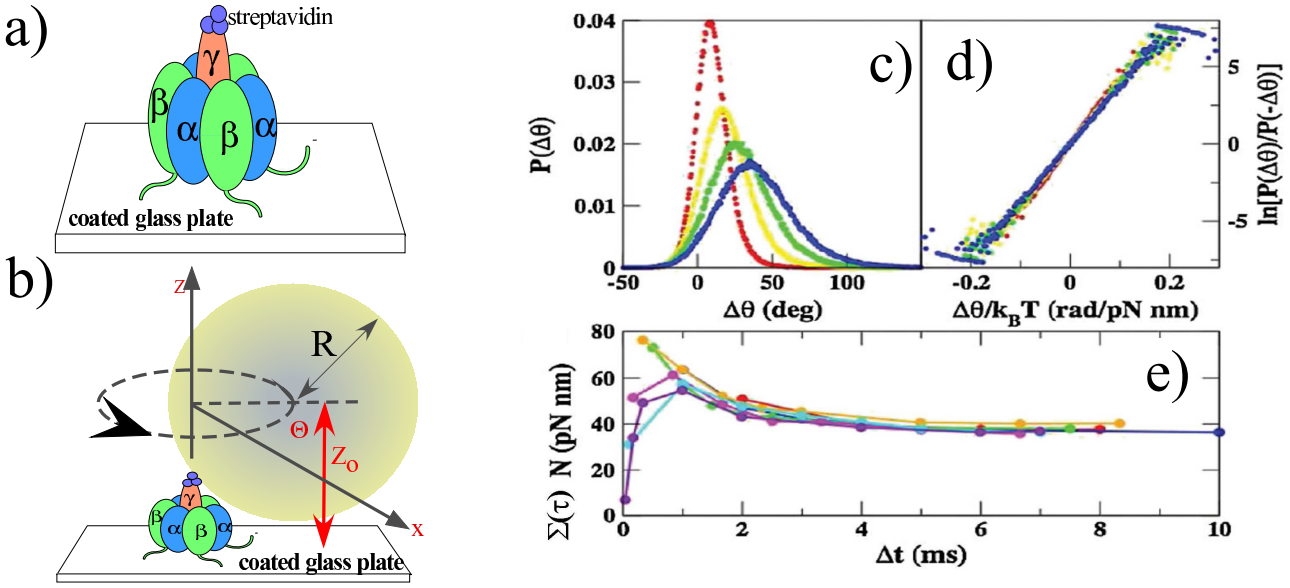

Figure 15: Molecular motor. a) Schematic diagram of a F_1-ATPase molecular motor composed by a rotor γ (radius ~ 1 nm) which rotates inside stator of radius ~ 5 nm formed by three α β subcomplexes. Sequential chemical reactions between the stator and the rotor produce the motion. The $\alpha\beta$ subcomplexes are attached to a suitably coated glass plate. Streptavidin is used to attach to γ either actin filaments [58] or streptavidin-coated beads [57]. b) In order to follow the rotation of the rotor with a standard microscope a streptavidin-coated bead of radius ~ 0.5 μm is glued to γ subunit (drawing not to scale). The figures c),d) and e) (taken from ref.[57])) illustrate the results of a measure. c) Pdfs for several τ of $\Delta\theta_\tau$. d) Symmetry function extracted from the Pdfs of c). e) Slopes $N\Sigma(\tau)$ of the symmetry function as a function of τ. The different colors pertain to different experimental conditions. Notice the convergency to an unique value of N for large τ. Strictly speaking in this figure the function $\Sigma(\tau)$ keeps into account also the fact that eq.27 is not necessarily valid for short times (see text)

5.1 Measuring the power of a molecular motor

A molecular rotary motor, as any kind of motor, is constituted by a stator and a rotor. The movement of the rotor is provoked by chemical reactions occurring sequentially between the rotor and stator. A typical example of bio-motor is the bacterial flagellum. However it has been shown [58] that a single molecule of F_1-ATPase may act as a motor composed by a γ subunit (radius ~ 1 nm) which rotates inside a barrel of radius ~ 5 nm formed by three α β subcomplexes (see fig.15a) for a schematic diagram and ref.[57, 58] for more details). In experiments, the $\alpha\beta$ subunit is stuck on a suitably activated glass plate as shown in fig.15a). The measure of the torque of this motor is important in order to know its efficiency as a function of the concentration of the chemicals contained in the liquid surrounding it. The typical size of this molecular motor is several nanometers and the moving unit is too small to be observed with an optical microscope. Therefore to measure the torque of F_1-ATPase motor a streptavidin-coated bead of radius 0.5 μm is glued on the subunit γ, and the motion of this bead is followed by a standard microscope as sketched in Fig. 15b). The motion of the bead occurs on a torus and θ is the coordinate of the motion along the torus. The time evolution of θ can be described by a Langevin equation:

$$\Gamma\ \dot{\theta} = N + \xi, \tag{27}$$

where N is the torque of the motor, Γ the viscous dissipation of the fluid surrounding the bead and ξ the thermal noise. In order to estimate N, it is in principle enough to measure the mean angular velocity $< \dot{\theta} >$ of the bead and obviously from eq.27 one gets:

$$N = \Gamma\ < \dot{\theta} > \tag{28}$$

However the procedure is not so simple because in order to estimate N one has to know the exact value of Γ, which is a function of the viscosity of the fluid, the radius L of the bead path, the radius R of the bead, the shape of the bead and the distance Z_o of the bead from the surface of the glass plate where the experiment is performed (see Fig. 15b). The variable Z_o is certainly the most difficult to be determined experimentally. Therefore using eq.28 the error on N can be really very large. There is instead another method proposed in ref.[3] for electric circuits and first used for measurements in bio-motors in ref.[57]. This method is based on work fluctuations and is much more precise. To apply it, we suppose that N is constant. This is a quite reasonable hypothesis for certain regimes of F_1-ATPase motors. We compute the work W_τ performed by the motor in a time τ:

$$W_\tau(t) = \int_t^{t+\tau} N\ \dot{\theta}(t)\mathrm{d}t = N\ \Delta\theta_\tau \tag{29}$$

where $\Delta\theta_\tau = \theta(t+\tau) - \theta(t)$ and we have used the fact that N is constant. In previous section we have seen that Langevin systems satisfy the SSFT, which we now apply to W_τ. Using eq.29 and the constancy of N SSFT for the molecular motor reads:

$$\ln\left(\frac{P(\Delta\theta_\tau)}{P(-\Delta\theta_\tau)}\right) = \Sigma(\tau)\ N\ \frac{\Delta\theta_\tau}{k_B T} \qquad \text{with}\ \ \Sigma(\tau) \to 1\ \ \text{for}\ \ \tau \to \infty \tag{30}$$

This equation is quite interesting because the value of N can be determined only by the measure of the fluctuations of $\Delta\theta_\tau$. Indeed plotting $\ln(P(\Delta\theta_\tau)/P(-\Delta\theta_\tau))$ as a function of $\Delta\theta_\tau/(k_B T)$ we notice that the slope of the straight lines is $\Sigma(\tau)\ N$. Therefore studying the asymptotic value of this slope for large τ one can determine N. It is interesting to note that in this case the knowledge of Γ is not needed. This technique has been recently applied to molecular motor in ref.[57] and their main results are plotted in Figs. 15 c),d),e). The relevant parameter $\Sigma(\tau)\ N$, extracted from the pdf of $\Delta\theta_\tau$ (Fig. 15 c) and the symmetry function (Fig. 15 d), is plotted in Fig. 15e) [3]. We see a clear convergence to a unique value and one gets a very precise estimation of the torque of the molecular motor independently of the size and shape of the bead glued to γ unit of the F_1-ATPase motor. This is a very specific and interesting example of the possible applications of FT.

6 The chaotic systems

In previous sections we have studied the probability of the instantaneous negative entropy production rates within the context of the FTs for stochastic systems, where the fluctuations are produced by the coupling with a thermal bath. In sec. 3.2 we have seen that when the energy injected into the system is larger than $100\ k_B T$ the probability of these negative events is very small and the time needed to observe them becomes extremely long. In other words the role of thermal fluctuations becomes negligible.

However in the introduction we have shown that instantaneous negative entropy production rates can be observed in chaotic systems such as, for example, turbulence and granular media, where the fluctuations are produced by the non linear interactions of many degrees of freedom. We have also pointed out that for chaotic systems the amount of injected energy is order of magnitudes larger than $k_B T$ and of course thermal fluctuations

[3] It has to be stressed that in this specific case $\Sigma(\tau)$ keeps into account the fact that for short time eq.27 is not a good approximation for the dynamics of the motor and eqs.29,30 apply only for long time

do not play any role in the fluctuating dynamics. The question that we want to analyze in this section is whether we can apply in these systems the FTs defined in sec.3 for stochastic systems, eqs.10-13. For a dissipative chaotic system one could imagine to replace k_BT, in eqs.10-13, with a characteristic energy E_c which keeps into account the relevant energy scales of the system fluctuations. However the definition of this relevant energy scale can be in general difficult and even impossible, because it may depend on the observable and on the kind of forcing. Thus the approach of introducing an E_c is not very useful to compare the experimental results with the proof given for dynamical systems [25]. Indeed in this case the theorem considers a quantity :

$$y_\tau = \frac{\sigma_\tau}{<\sigma_\tau>} = \frac{\int_t^{t+\tau} \sigma(t)\,\mathrm{d}t}{<\sigma_\tau>} \tag{31}$$

where $\sigma(t)$ is the instantaneous phase space contraction rate, σ_τ the integral of σ on a time τ and $<\sigma_\tau>$ the mean of σ_τ. Three hypothesis has been done on the dynamical system which must be : a) dissipative, b) time reversible c) Anosov [4]

$$\frac{1}{\tau}\ln\frac{P(y_\tau)}{P(-y_\tau)} = <\sigma> y_\tau + O(1/\tau) \quad \text{for} \quad \tau \to \infty \tag{32}$$

where $<\sigma>$ is the mean phase space contraction rate, which has the dimension of $1/t$. In this equation the relevant variable is the phase space contraction rate which has been identified as the entropy production rate[25]. The phase space contraction rate is a global variable of the system but an extension of the theorem for local variables has been done in refs.[55, 56]. One reason for developing local FT is that global fluctuations are usually not observable in macroscopic systems, as a consequence it is important to understand whether a local measurement is representative of the dynamics. Eq.32 has been tested in several numerical simulations (see for example ref.[33, 34] for a review), here we want to focus on experiments.

6.1 Experimental test

The test of eq.32 in experiments is extremely useful to analyze several important questions. The first one is whether eq.32 may have a more general validity independently of the restrictive hypothesis done to prove it. Indeed the hypothesis b) is never satisfied in real systems and the hypothesis c) does not necessarily apply to all of them. Thus in general we do not even know whether eq.32 can be applied in the experimental system under study. The second question concerns the choice of the observable. Indeed the direct measure of the phase space contraction rate is not possible and one has to rely upon the measure of another observable usually the energy W_τ injected into the system by the external forces in a time τ. In other words one is making the important hypothesis that y_τ, defined in eq.31 in terms of $\sigma(t)$ is equivalent to $x_\tau = W_\tau/ < W_\tau >$. This hypothesis, that is not necessarily valid, is the second question that one would like to address in experiments. The third question is related to the estimation of the prefactor $<\sigma>$ in the right hand side of eq.32. This prefactor, which is a function of the Lyapunov exponents, is very difficult to estimate in an experimental system. Finally the last question concerns the relevance of a local observable to characterize the dynamics of the system.

There are not many experiments where these questions have been analyzed in some details. In several experiments [4, 36] only the linearity in x_τ of the symmetry function $\rho(x_\tau) = (1/\tau)\ln\left(P(x_\tau)/P(-x_\tau)\right)$ has been checked, which, for the reasons discussed in the previous paragraph, is only a partial test. For example three experiments have tried to give an answer to the question of the prefactor. Two of these experiments are performed in granular media [5, 6] and the third on mechanical wave turbulence in a metallic plate[63]. We will not describe in details the experiments here but we will comment the main results.

6.1.1 *Granular media*

The two experiments of refs.[5, 6] consist of diluted granular media strongly shaken by a vibrator, but the measured quantities are not the same. In ref.[5] the authors measure the fluctuations of the energy flux in a

[4] For a precise definition see refs.[35, 34]. Roughly speaking this property ensures that the system is chaotic and that on the attractor there are no regions of finite volume that do not contain points.

subvolume of the system. Instead ref.[6] the work done by an external force on a ratchet inside the granular media is measured. They both find that although the system is not thermal the stochastic version of SSFT (eq.10) holds, provided that k_BT is replaced by a characteristic energy E_c:

$$\ln \frac{P(x_\tau)}{P(-x_\tau)} = \frac{< X_\tau >}{E_c} x_\tau + O(1/\tau). \tag{33}$$

with $x_\tau = X_\tau / < X_\tau >$, X_τ is the integral of energy flux in ref.[5] and the work W_τ performed by an external force on a ratchet in ref.[6]. It must be pointed out that in both experiments of refs.[5, 6] the energy E_c has been measured independently. In ref.[5] is found that E_c is about 5 times larger than the kinetic energy K_E of the shaken granular medium for all the values of the control parameters used in the experiment. The fact that K_E and E_c have the same dependence on the control parameter have been interpreted considering that the vibrator injects into the system the amount of energy lost in the collisions but once excited in a NESS the granular medium behaves like a thermal bath for the measured observable. However this interpretation is not necessarily correct. Indeed for the experiment of ref.[5] it as been shown in a numerical simulation [59] that for the quantity measured in this experiment FT does not apply for the large deviations x_τ because the symmetry function $S(x_\tau)$ becomes non-linear for large x_τ. This discrepancy between theory and experiment is obviously coming from the fact that experimentally the very large deviation are difficult to be measured, thus the non-linear part of $S(x_\tau)$ cannot be observed. However the experiment of ref.[5] is certainly interesting because is the first where the question of the prefactor has been analyzed experimentally. In contrast for the experiment of ref.[6] is observed that $E_c = K_E(1+\alpha)/2$ where α is the restitution coefficient of the grains. It is interesting to notice that $K_E(1+\alpha)/2$ is the temperature of an intruder inside a diluted granular gas as it has been found in theoretical models [60, 61, 62]. These two examples of comparison between numerical and experimental results show the difficulty of interpreting the experimental results on FT and the importance of verifying them in a precise theoretical framework. Where does the difference between the experiments of ref.[5] and ref.[6] come from ? The answer can be found on the fact that in the two experiments two different quantities are measured. Indeed in sect.3 we have seen that, even for stochastic systems, the fluctuations of W_τ, Q_τ and $\Delta s_{\mathrm{tot},\tau_\mathrm{n}}$ behave differently within the context of FT. This can be more complex for granular media and it will be useful to give more insight on this point. Furthermore even in cases where a description in terms of Ec applies, comparing eq.33 with eq.32 a question that arises naturally is whether $< W_\tau > /E_c$ is a good estimation of $< \sigma > \tau$. This is an important question which will be interesting to analyze in the future.

6.1.2 *Mechanical waves*

In the experiment on mechanical waves[63], a metallic plate is set into a chaotic state of wave turbulence by a periodic local forcing at 75 Hz. (see Fig. 16a). The chaotic dynamics is produced by the non-linear interaction of the oscillatory modes of the plate. The authors measure the local force and displacement (see Fig. 16a) and compute the work W_τ done on a time τ by the external force which excites the vibrations of the plate. They find that the pdfs of $x_\tau = W_\tau / < W_\tau >$ are strongly non-gaussian (see Fig. 16b). From these pdfs they compute the symmetry function $\rho(x_\tau)$ which is plotted (see Fig. 16c) as a function of x_τ. We see that in spite of the fact that the pdf are not Gaussian the function $\rho(x_\tau)$ (Fig. 16c) converges to a unique straight line for large τ as predicted by FT. From eq.32 the slope of this straight line is $< \sigma >$, which the authors can estimate independently by measuring the relaxation time of the vibrational modes. They find that the values estimated with the two methods (FT and the relaxation time) are very close and within experimental errors. This result is quite interesting and it is probably the only experiment where a direct test of eq.32 has been done. Certainly the errors of this comparison are very large but this kind of tests are useful to understand in some details the applications of FTs to chaotic systems.

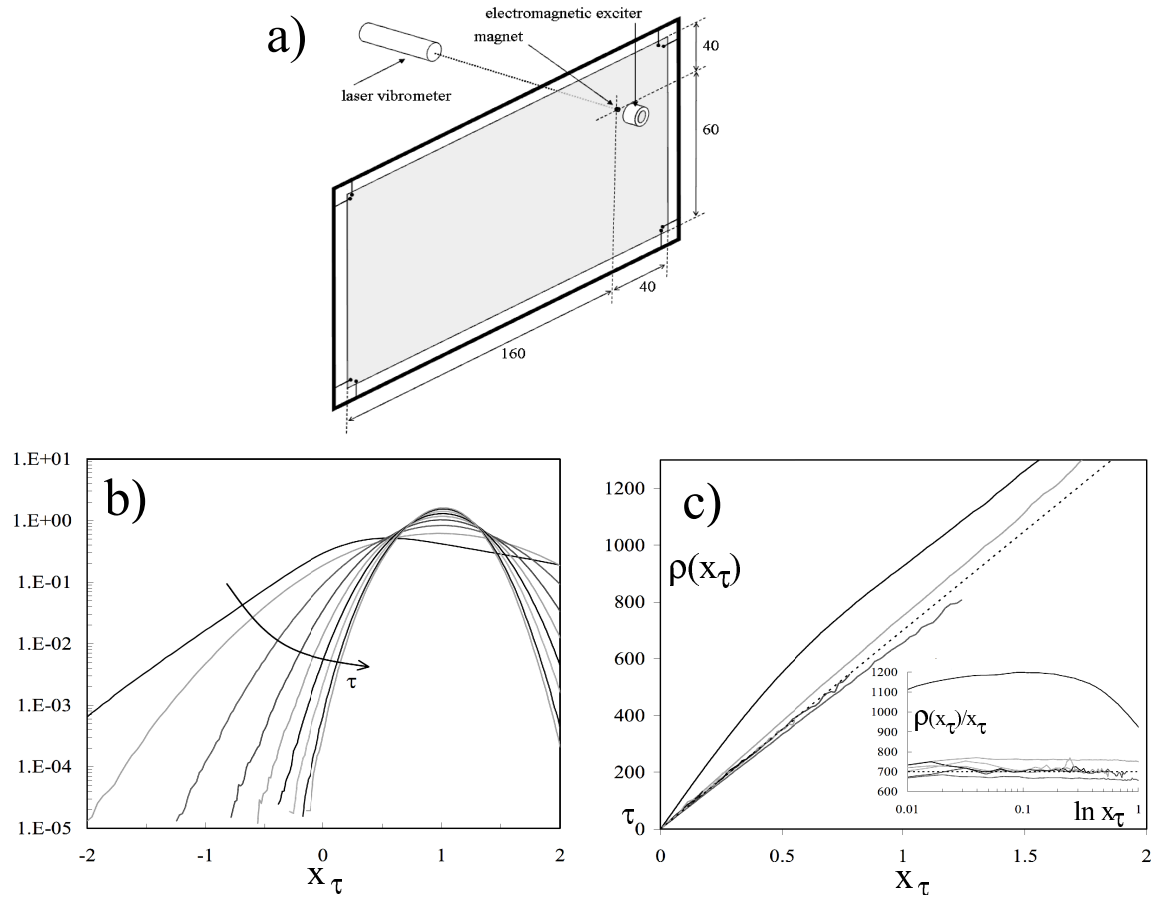

Figure 16: Mechanical waves in a metallic plate (from ref.[63]). a) Schematic diagram of the experiment. A steel plate is suspended to the frame. Dimensions are in cm. The electromagnetic exciter produce et local forcing of the plate vibrations. A laser vibrometer measures the normal velocity at the excitation point. b)and c) Results on the periodic forcing. (b) Pdfs of the injected power on the time durations of τ for $\tau = 3.5ms,\ 6.5,\ 13.5,\ 20,\ 26.5,\ 33.5,\ 40,\ 47.5,\ 52ms$) (c) Functions $\rho(x_\tau) = (1/\tau)\ln\left(P(x_\tau)/P(-x_\tau)\right)$ obtained from the Pdfs of (b). Inset: compensated value $\rho(x_\tau)/x_\tau$ in a semi log plot. In (c) the dashed line corresponds to a linear law of slope $< \sigma >= 700Hz$.

7 Summary and concluding remarks

In this paper we have reviewed several experimental results on the fluctuations of injected and dissipated power in out of equilibrium systems. We considered the two cases when the fluctuations are produced by the coupling with the heat bath (stochastic systems) and when they are produced by the non linear interactions of many degrees of freedom (chaotic systems). We have seen that in both cases we observe that the external forces may produce a negative work because of fluctuations. The probability of these negative events has been analyzed in the framework of fluctuation theorem.

We have mainly discussed the stochastic systems described by Langevin equations, both with harmonic and unharmonic potential. We have seen that injected and dissipated power present different behaviors. FTs are valid for any value of W_τ whereas can be applied only for Q_τ $<< Q_\tau >$ in the case of the heat. We have also seen the the finite time corrections to SSFT depend on the driving and on the properties of the system. We have introduced the total entropy, which takes into account only the entropy produced by the external forces neglecting the the equilibrium fluctuations. For the total entropy FTs are valid for all the times. We discussed the applications of FTs to extract important physical properties of a stochastic system. Thus one may

conclude that for Markovian systems driven by a deterministic force the applications of FT does not present any major problems and can be safely applied. The case of random driving has been recently discussed and several problems may arise when the variance of the driving become larger than the fluctuations induced by the thermal bath. We have not discussed this problem but an analysis of this specific case can be found in refs.[8, 64, 65].

Finally we discussed the applications of FT to chaotic systems. The experimental test is in this case very important and useful because many questions can be asked on the system under study which does not necessarily verify all the theoretical hypothesis. One has to say that in the case of non-Gaussian statistics even the linearity of the symmetry function can be an interesting result. However we pointed out that, for a real comparison with theory, the difficulty is to estimate of the prefactor of eq.32 by an independent measurement. Only a few experiments have addressed this point in some details, but many problems remain open and it seems to be difficult to find a general behavior for chaotic systems as for the case of stochastic ones.

Acknowledgements

Several results reviewed in this article has been obtained in collaboration, with L. Bellon, R. Gomez-Solano, N. Garnier, P. Jop. We acknowledge useful discussions and collaboration during the past ten years with D. Andrieux, E. Cohen, R. Chetrite, G. Gallavotti, P. Gaspard, K. Gawedzky and A. Imparato. We thank A. Puglisi and E Trizac for useful comments on FT in granular media. We are grateful to H. Noji, K. Hayashi and A Boudauoud for having allowed us to reproduce the figures of their articles in the present one.

References

[1] C.W. Chang, D. Okawa, H. Garcia, A. Majumdar and A. Zettl, Phys. Rev. Lett.101, 075903 (2008)

[2] R. van Zon, S. Ciliberto, E. G. D. Cohen, Phys. Rev. Lett. 92 (13) 130601 (2004)

[3] N. Garnier, S. Ciliberto, Phys. Rev. E 71 060101(R) (2005).

[4] S. Ciliberto, N. Garnier, S. Hernandez, C. Lacpatia J. -F. Pinton, G. Ruiz Chavarria, Physica A 340, 240 (2004).

[5] K. Feitosa, N. Menon, Phys. Rev. Lett. 92 164301 (2004).

[6] S. Joubaud, Talk at STATPHYS24, (Cairns 2010). Abstract, Topic 3: http://www.statphys.org.au/.

[7] A. Kis Andras and A. Zettl, Phil.Trans. of the Royal Society A: Mathematical, Physical and Engineering Sciences, 366, 1591, (2008).

[8] J. R. Gomez-Solano , L. Bellon , A. Petrosyan and S. Ciliberto, Europhys. Lett., 89, 60003 (2010).

[9] L.Bellon, L. Buisson, S. Ciliberto, F. Vittoz, Rev. Sci. Instrum., 73 (9), 3286,(2002).

[10] L. Bellon and S. Ciliberto, Physica D 168, 325 (2002)

[11] H. Lamb, Hydrodynamics, 6^{th} ed., Dover Publication, 1945, republication of the 1932 ed., Cambridge University Press.

[12] L. Bellon, S. Ciliberto, H. Boubaker et L. Guyon, Optics Communications, 207, 49-56 (2002).

[13] F. Douarche, S. Ciliberto, A. Petrosyan, J. Stat. Mech. p09011 (2005).

[14] F. Douarche, S. Joubaud, N. Garnier, A. Petrosyan, S. Ciliberto, Phys. Rev. Lett. 97 140603 (2006).

[15] F. Douarche, L. Buisson, S. Ciliberto, A. Petrosyan, Rev. Sci. Instr. 75 (12) 5084 (2004).

[16] S.Joubaud, N. B. Garnier, F. Douarche, A.Petrosyan, S. Ciliberto, C.R. Physique, special issue: "Work, dissipation, and fluctuations in nonequilibrium physics", Editors: B. Derrida, P. Gaspard, C. Van den Broeck. (Elsevier 2007); cond-mat/0703695

[17] S. Joubaud, N. B. Garnier, S. Ciliberto, J. Stat. Mech., P09018,(2007).

[18] V. Blickle, T. Speck, L. Helden, U. Seifert, and C. Bechinger, Phys. Rev. Lett. 96, 070603 (2006).

[19] S. Schuler, T. Speck, C. Tietz, J. Wrachtrup, and U. Seifert, Phys. Rev. Lett., 94, 180602 (2005).

[20] F. Zamponi, F. Bonetto, L. Cugliandolo, J. Kurchan, J. Stat. Mech. p09013 (2005).

[21] Sekimoto K, Progress of Theoretical Phys. supplement (130), 17 (1998).

[22] T. Hatano, S. Sasa, Phys. Rev. Lett, 86, 3463 (2001).

[23] D. J. Evans, E. G. D. Cohen, and G. P. Morriss, Phys. Rev. Lett. 71, 2401 (1993);

[24] D. J. Evans and D. J. Searles, Phys. Rev. E 50, 1645 (1994). D. J. Evans, D. J. Searles, Advances in Physics 51 (7) 1529 (2002). D. J. Evans, D. J. Searles and L. Rondoni, Phys. Rev. E 71 (5) 056120 (2005).

[25] G. Gallavotti and E. G. D. Cohen, Phys. Rev. Lett. 74, 2694 (1995); G. Gallavotti and E. G. D. Cohen, J. Stat. Phys. 80(5-6), 931 (1995).

[26] J. L. Lebowitz and H. Spohn, J. Stat. Phys. 95, 333 (1999).

[27] J. Kurchan, em J. Phys. A, Math. Gen. 31, 3719 (1998);

[28] J. Farago, J. Stat. Phys. 107 781 (2002); Physica A 331 69 (2004).

[29] R. van Zon and E. G. D. Cohen, Phys. Rev. Lett. 91 (11) 110601 (2003); Phys. Rev. E 67 046102 (2003); Phys. Rev. E 69 056121 (2004).

[30] D. J. Searles, L. Rondoni, D. J. Evans, J. Stat. Phys. 128, 1337 (2007).

[31] U. Seifert,Phys. Rev. Lett., 95, 040602 (2005).

[32] A. Puglisi, L. Rondoni A. Vulpiani, J. Stat. Mech.: Theory and Experiment, P08010, 2006)

[33] L. Rondoni and C. Meíja-Monasterio, Nonlinearity 20, R1(2007)

[34] F. Zamponi,J. Stat. Mech., P02008 (2007)

[35] G. Gallavotti, F. Bonetto, and G. Gentile.*Aspects of the ergodic, qualitative and statistical theory of motion* Springer Verlag, Berlin, 2004.

[36] S. Ciliberto and C. Laroche, J. Phys. IV, France 8, 215 (1998).

[37] G. M. Wang, E. M. Sevick, E. Mittag, D. J. Searles, D. J. Evans, Phys. Rev. Lett. 89 050601 (2002); G. M. Wang, J. C. Reid, D. M. Carberry, D. R. M. Williams, E. M. Sevick, D. J. Evans, Phys. Rev. E 71 046142 (2005).

[38] T. Speck, U. Seifert, Eur. Phys. J. B 43, 521 (2005).

[39] S.Joubaud, N. Garnier, S. Ciliberto, Eur. Phys. Lett. 82, 30007 (2008).

[40] P.Jop, S. Ciliberto, A. Petrosyan, Eur. Phys. Lett. 81, 5 (2008) 50005

[41] R.Benzi,G. Parisi, A. Sutera,A. Vulpiani, SIAM J. Appl. Math., 43, 565 (1983).

[42] L. Gammaitoni, F. Marchesoni and S. Santucci. Phys. Rev. Lett. 74 (7), 1052-1055 (1995).

[43] C. Schmitt, B. Dybiec, P. Hänggi and C. Bechinger. Europhys. Lett. 74 (6), p. 937 (2006)

[44] T. Iwai. Physica A 300, pp. 350-358 (2001)

[45] D. Dan and A. M. Jayannavar. Physica A 345, pp. 404-410 (2005)

[46] A. Imparato, P. Jop, A. Petrosyan, S. Ciliberto, J. Stat. Mech. (2008) P10017

[47] C. Jarzynski, Phys. Rev. Lett. 78 (14), 2690 (1997)

[48] C. Jarzynski, J. Stat. Phys. 98 (1/2), 77 (2000)

[49] G.E. Crooks, Phys. Rev. E 60 (3), 2721 (1999)

[50] F. Ritort, Séminaire Poincaré 2, 63 (2003)

[51] J. Liphardt, S. Dumont, S.B. Smith, I. Ticono Jr., C. Bustamante, Science 296, 1832 (2002)

[52] J. Prost, J-F Joanny, J. M. R. Parrondo, Phys. Rev. Lett. 103, 090601 (2009)

[53] A. Crisanti and F. Ritort, Europhys. Lett. 66, 253 (2004).

[54] P. Jop , R. Gomez Solano, A. Petrosyan, S. Ciliberto, J. Stat. Mech. P04012, (2009).

[55] Gallavotti G, J. Phys. A: Math. Gen. 263, 39 (1999).

[56] G. Ayton, D. J. Searles, D. J. Evans, J. Chem. Phys. 115, 2033 (2001).

[57] K. Hayashi, H. Ueno, R. Iino, H. Noji, Phys. Rev. Lett. 104, 218103 (2010)

[58] H. Noji, R. Yasuda, M. Yoshida, and K. Kinosita, Jr., Nature 386, 299 (1997).

[59] A. Puglisi,P. Visco, A. Barrat, E. Trizac, F. van Wijland, Phys. Rev. Lett 95, 110202 (2005)

[60] A. Sarracino,D. Villamaina, G. Costantini, A. Puglisi, J. Stat. Mech. , (2010) P04013

[61] G. Costantini, U. Marini Bettolo Marconi and A. Puglisi , Phys. Rev. E, **75**(6) 061124 (2007)

[62] B. Cleuren and C. van den Broeck, *Europhys. Lett.*, (2007) **77** 50003

[63] O. Cadot, A. Boudaoud, C. Touz, EPJ B 66, 399 (2008).

[64] A. Baule, E. Cohen, Phys. Rev. E, 80, 011110 (2009).

[65] M. Bonaldi et al., Phys. Rev. Lett. 103, 010601 (2009).